J. Phys. E: Sci. Instrum., Vol. 17, 1984. Printed in Great Britain

P-1187-1132 (6) E P.D: 12/1984

A simultaneous angle-resolved photoelectron spectrometer

A Bosch, H Feil and G A Sawatzky
Department of Physical Chemistry of the Material Science Center, University of Groningen, Nijenborgh 16, 9747 AG Groningen, The Netherlands

Received 10 April 1984, in final form 21 June 1984

Abstract. We show how a double pass cylindrical mirror analyser can be modified for use as a simultaneous angle-resolved photoelectron spectrometer. The full acceptance cone of the analyser is imaged on a two-dimensional position sensitive detector. The position information is stored in a two-dimensional multichannel analyser. The spectrometer accumulates multiple angle-resolved spectra simultaneously. Its energy resolution is determined as 0.9% FWHM and the angle-resolving capability is demonstrated with valence band spectra from Ag(111), giving an angular resolution in the present set-up of about two degrees.

1. Introduction

Angle-resolved photoelectron spectroscopy is one of the most direct techniques for the study of the electronic structure of solids. The experimental peak positions of photoemitted valence band electrons can be related to the theoretical bandstructure via the electron-emission geometry at the surface and the symmetry properties in the angular intensity distributions. Another field of application is the study of the electronic structure of adsorbed species. Photoelectron spectroscopy can give valuable information about the orientation and chemical interactions of adsorbed molecules on solid surfaces.

As the technique is surface sensitive because of the small electron escape depth, the surface conditions should be kept absolutely constant during the measurement. This requires a fast measuring scheme and has stimulated the development of imaging electron spectrometers in which a number of emission angles can be monitored simultaneously. Such a spectrometer is developed by Eastman and co-workers (1980), using the retarding field analyser. Because of a better energy resolution a cylindrical mirror analyser (CMA) is applied in our set-up. We will show below that in combination with a high-resolution position sensitive detector, placed behind the exit diaphragm, a versatile instrument can be obtained in which a fairly large range of angles can be selected electronically without any mechanical motion. This use of the CMA can be contrasted to other solutions, like that by Harting (1971) who used fixed slits or Niehus and Bauer (1975) who obtained angular dependence by placing a cylindrical aperture in front of the analyser. Commercially the CMA is available with a rotating drum inside the inner cylinder (see for instance Baird 1981). Our solution is similar to that by van Hoof and van der Wiel (1980) in the sense that a position sensitive detector is placed at the analyser exit. These authors used however a discrete detector and obtained relatively low intensities. In our spectrometer we combine the CMA and detector with a two-dimensional multichannel analyser (MCA), which provides for a fast measuring scheme.

In the next section, the relevant properties of the CMA are reviewed. In § 3 the experimental set-up is described and § 4 presents the experimental results. Finally, some conclusions are given in § 5.

2. Properties of the CMA

The electron–optical properties of the CMA are described in several articles by Zashkvara *et al* (1966), Sar-El (1968), Aksela *et al* (1970), Eagen and Sichafus (1977) and Draper and Lee (1977). We only review here those properties that are relevant for the present work.

Although an experimental version of the instrument is reported as early as 1952 by Gremmelmeier, the analyser is still subject to improvements. In our spectrometer, schematically shown in figure 1, we use a commercial double-pass analyser (PHI model 12-250). The application of this instrument for Auger spectroscopy and ESCA is described by Palmberg (1974). The spectrometer constant k is defined as $k=(T/V)\ln(b/a)$, where T and V are respectively the electron kinetic energy and the potential difference across the two cylinders; a and b are respectively the radius of the outer and inner cylinder. Taking $k=1.3098$, second order focusing is obtained for a point source on the CMA axis at a central entrance angle of 42.3°. The acceptance solid angle is a cone and has a width corresponding to the angular focusing. In a complete description of the electron trajectories however higher order terms and the effect of a finite source should be examined. The full analyser response function is calculated for instance by Draper and Lee (1977).

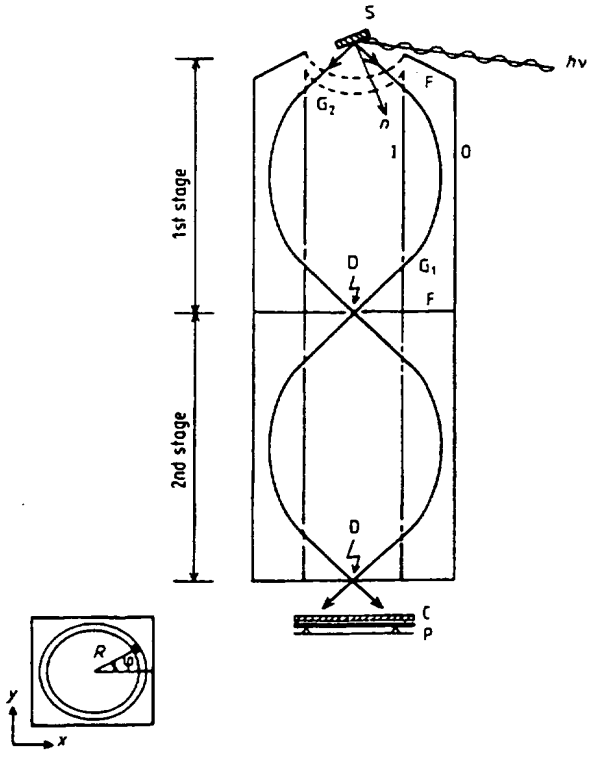

Figure 1. Two-stage CMA with position sensitive detector. The characters denote: I, (inner cylinder); O, (outer cylinder); F, (fringing plate); G_1, (cylinder grids on inner cylinder); G_2, (retarding spherical grids); D, (aperture); C, (double channel plate assembly); P, (position detector); S, (sample).

The obtainable resolving power depends on the energy dispersion $T\partial T/\partial L$ (L is the length of the projection of the electron trajectory on the CMA axis) and on the axial spread of

0022-3735/84/121187 + 06 $02.25

the image at the detection aperture. The dispersion of the analyser can be increased by multi-stage focusing (Zashkvara *et al* 1966), however with subsequent loss in sensitivity. The spread of the image with respect to the source is mainly due to the finite source and aberration effects. The image can be reduced to true dimensions by using an appropriate aperture stop at the exit.

The four cylindrical grids attached onto the inner cylinder wall will affect the analyser operation physically by reducing the transmission. In addition field penetration through the meshes of the grids yields a lower experimental resolution than is calculated theoretically. To enhance the transmission we have replaced the delivered grids by etched molybdenum grids (Buckbee–Mears Comp.) with 97% transmission. They were attached to the inner cylinder wall with two component silver epoxy, which does not affect the base vacuum after bake-out. The analyser performance is further improved by coating all metal parts with graphite (Acheson Daq 386) which improves the resolution and reduces strongly the secondary background at low energies.

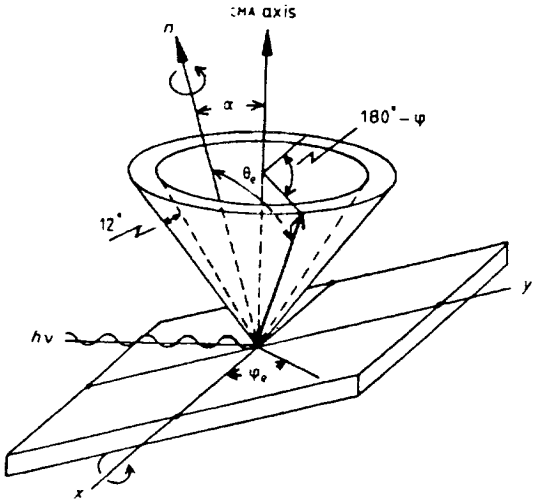

Figure 2. Geometry of the sample surface coordinate system and the CMA acceptance cone. The sample is rotated by α around the x axis. θ_e and φ_e are exit angles at the sample. R and φ are the coordinates in the detector plane (see figure 1).

For a discussion of the angular properties we use figure 2 where the acceptance solid angle with central cone angle of 42.3° is shown. Because of the symmetry of the electron trajectories in the CMA, the incoming and outgoing electrons have the same direction of propagation and a conical distribution of electrons is present at the analyser exit. In the normal set-up an electron multiplier is placed at the exit which integrates over the acceptance cone. If, however, a flat position sensitive detector is used behind the 2nd stage exit aperture, see figure 1, the conical acceptance solid angle is imaged as a circle. The divergence of the incident beam gives a correspondent width to the circular image at the detector. It is clear from figure 1 that every direction of propagation of an incoming electron within the acceptance solid angle corresponds to a unique position at the detector. By recording the position of electrons striking the flat detector in the circular image angle-resolved electron spectroscopy is feasible. But also the full image can be exploited by recording the intensities from all positions at the detector as a function of kinetic energy, which results in a simultaneous multiple angle detection system. This requires fast position determination and storage of the events at the detector (see below).

The geometry is described using the angles θ_e and φ_e for the polar and azimuthal angles of the wavevector of the emitted electron with respect to the coordinate system of the sample surface, see figure 1. In the plane of the detector we use the polar coordinates R and φ. The angles are related via the equations

$$\cos\theta_e = -\sin\alpha\sin(42.5°)\sin\varphi + \cos\alpha\cos(42.3°)$$

$$\sin\varphi_e\sin\theta_e = \sin(42.3°)\cos\varphi$$

where a possible positive rotation α around the x axis is introduced. When $\alpha = 0$, $\theta_e = 42.3°$ at every φ and only azimuthal dependence is left. For $\alpha = 42.3°$, the surface normal is directed along the analyser acceptance cone and almost the full polar range is accessible using the rotation around the surface normal, i.e. $0 \leqslant \theta_e \leqslant 84.6°$. This is the geometry for performing normal photoemission. For other values of α, the angular range is limited. (It is noted that the angle of incidence of the light beam with respect to the sample surface varies when using the rotation α.)

In practice a further limitation is encountered. The grids on the inner cylinder wall are fixed by three vertical bars that physically prevent transmission along these lines. However by aligning the analyser properly this inconvenience can be limited.

3. Experimental set-up

The experimental apparatus is depicted schematically in figure 3. The flat two-dimensional position-sensitive detector (Surface Science Lab. Inc., SSL Model 239G) consists of two microchannel plates in series with a resistive anode detector. Electrons that pass the CMA are multiplied in the channel plates and the charge cloud is accelerated to the anode. The position of the centre of the charge cloud is determined using charge division to the four output terminals (Lampton and Carlson 1979). The detector has an active area of 25 mm diameter and a spatial resolution of 100 line pairs per inch, giving an uncertainty of $\Delta\varphi_e \simeq \pm 0.3$, $\Delta\theta_e \simeq \pm 0.1°$.

As the spectrometer is operated in the counting mode with count-rates up to $3 \times 10^4\ s^{-1}$, we use a fast two-dimensional multichannel analyser (Nuclear Data ND620), provided with 4096 channels. The analogue position output of the position analyser is digitised by two gated ADCs (ND575), that have a conversion time of $(2.1 + 0.0125\,N)\,\mu s$ (N is the channel number) at a conversion gain of 256. Detector and MCA present together a deadtime of about 13 μs.

The exit aperture of the CMA gives rise to angular uncertainties. In our geometry, with an aperture of 0.8 mm diameter, this results in $\Delta\varphi_e \simeq \pm 1.8°$, $\Delta\theta_e \simeq \pm 1.0°$.

As shown in figure 3, the operation of the complete spectrometer is controlled by an Apple II computer. For connection to the MCA we use a serial RS 232 communication board, which is modified to operate at 4800 baud. At the MCA side is a serial ND620 (70-2437) interface. This communication line is used for image processing and selection of angle-resolved spectra. Data storage is accomplished with two floppy disc units. The xy recorder is interfaced via a 10 bit DAC. Two outputs of the Game I/O of the Apple are used to program the reference voltage supply, which delivers a stepped reference voltage to control the analyser supply (NS, RST lines). The acquisition of angle-resolved spectra proceeds as follows. For a selected energy the MCA is set to acquire the full two-dimensional image during a certain time. The acquired intensity distribution is dumped into the computer and processed to obtain angle-resolved intensities. During processing the next energy is set and the acquisition is started. To prevent however large data files and long processing times, several precautions must be taken.

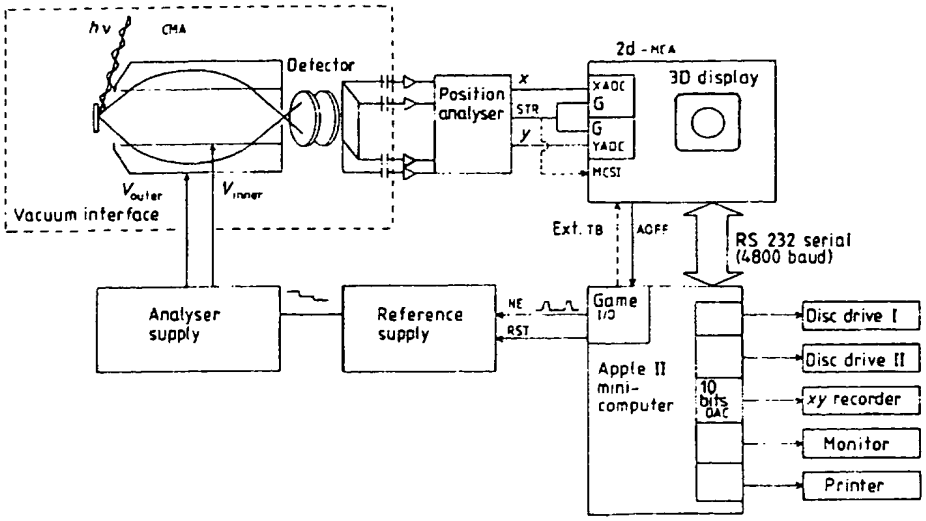

Figure 3. Schematic diagram of the experimental set-up. Explanations in the text. Of the CMA only one stage is shown.

In the first place, time can be saved by selecting from the two-dimensional field at the detector only the circular image region or more particularly only small segments of it corresponding to specific emission angles. For this purpose the MCA is programmed to deliver as output the intensities of the selected areas and limited datafiles have to be processed. Typically about six angle-resolved spectra are collected simultaneously within half an hour, which is demonstrated in our experiments on chemisorbed pyridine on silver (Bosch 1982). A disadvantage of this approach is that the full angular information available in the image still is not exploited.

A second way to circumvent long datafiles is to perform the calculation of the emission angle of every event at the detector in an analogue device connected to the x and y signals. The x and y values can be converted to R and φ values, see figure 1. We have recently modified the electronics to do this. The details of this modification and the results will be published elsewhere. Here we suffice by noting that the modification does eliminate the data-file problem without a loss in dead time or in angular resolution and in addition eliminates the necessity of a two-dimensional MCA.

The system can of course also be operated in the angle-integrated mode using the broken lines in figure 3. The UPS spectra are then directly accumulated in the MCA.

As is discussed above sample rotation and tilt are required to expand the angular range. For a CMA this is not simple because of the limited working space between the analyser and the sample surface (about 11 mm distance), which is fixed by the electro-optical properties. We designed a manipulator that is adapted to the CMA dimensions, see figure 4. Essential is that the basic manipulations are accomplished via the central shift of the rotary feedthrough B. This simplifies the design. In addition no translation tables are provided because we positioned the CMA on three mini rotary feedthroughs, by which its source point can be adjusted to the sample.

To avoid magnetic materials as much as possible, we

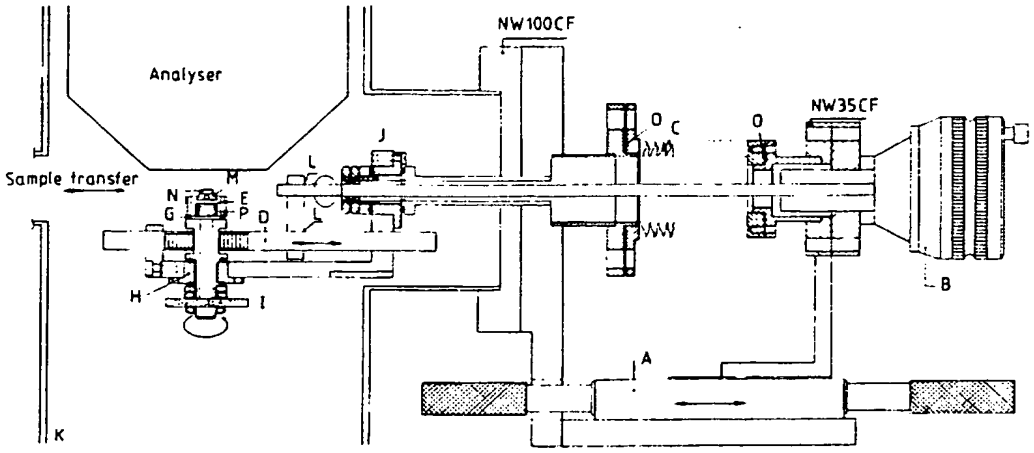

Figure 4. Cross section of the manipulator: A, (micrometer driven translation table); B, (rotary feedthrough); C, (membrane bellow); D, (rack); E, (sample table); G, (sapphire balls); H and J, (glass-ball bearings); I, (isolating ceramic disc); K, (vacuum chamber); M, (sample holder); N, (sample); O, (gold seal); L, (fixed cross connection). The rotations are indicated with arrows.

designed the couplings H and J using glass-ball bearings. To prevent hindrance by the thermocouple or heating wires (not shown), the sample table E with the sample holder M is placed on a hollow toothed shaft that rotates in H. The wires to the thermocoax windings inside the sample table and to the thermocouple, are inside this hollow shaft and connected to the ceramic disc I. From there they are connected to the feedthroughs on the flange. E is thermally isolated via three sapphire balls.

A rotation around the sample surface normal is accomplished with the translation table A. Via the fixed cross connections L and the toothed bar D, E is rotated. The gearing of rack and pinion is chosen carefully to achieve accuracy. We choose a pitch of 1.57 mm, giving 22 teeth at the given diameter of the hollow shaft. This results in 10.42° rotation for 1 mm translation. The tilt is accomplished by rotating the feedthrough B. Because D is fixed to move only in the indicated direction, the complete manipulator table rotates in bearings J. An advantage over other designs is that the angular range is high: 360° azimuthal and ±90° polar.

In the earlier stages of our experiments cooling was performed by means of the cooled tip of the sample transfer probe and a temperature was reached of about 150 K. Recently however the manipulator is provided with a He cooling system

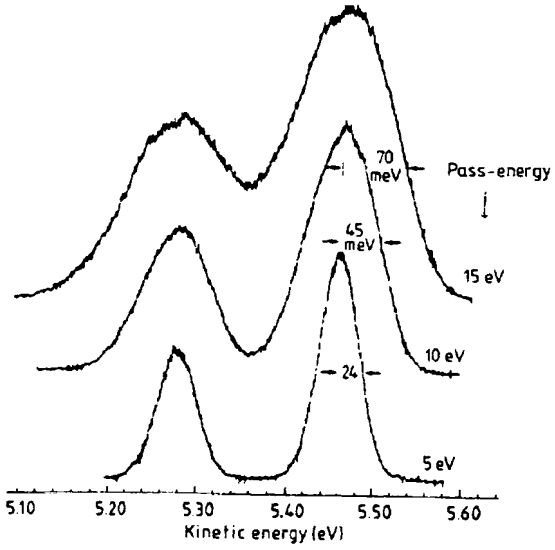

Figure 5. HeI spectra of the Ar3p lines at different pass-energies.

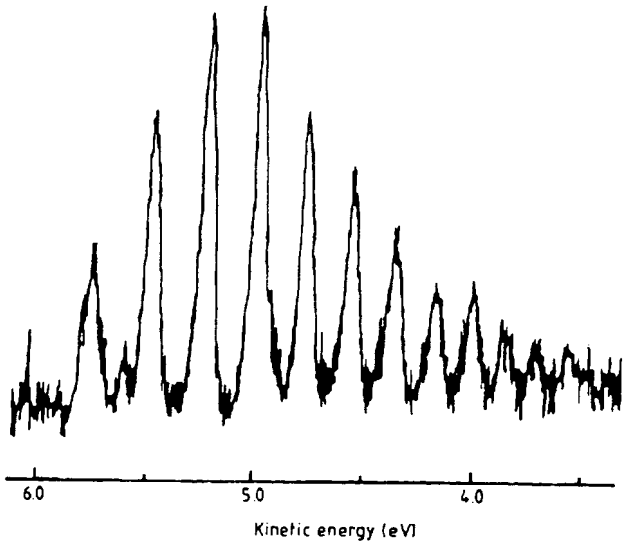

Figure 6. HeI spectrum of H_2 at 5 eV pass-energy.

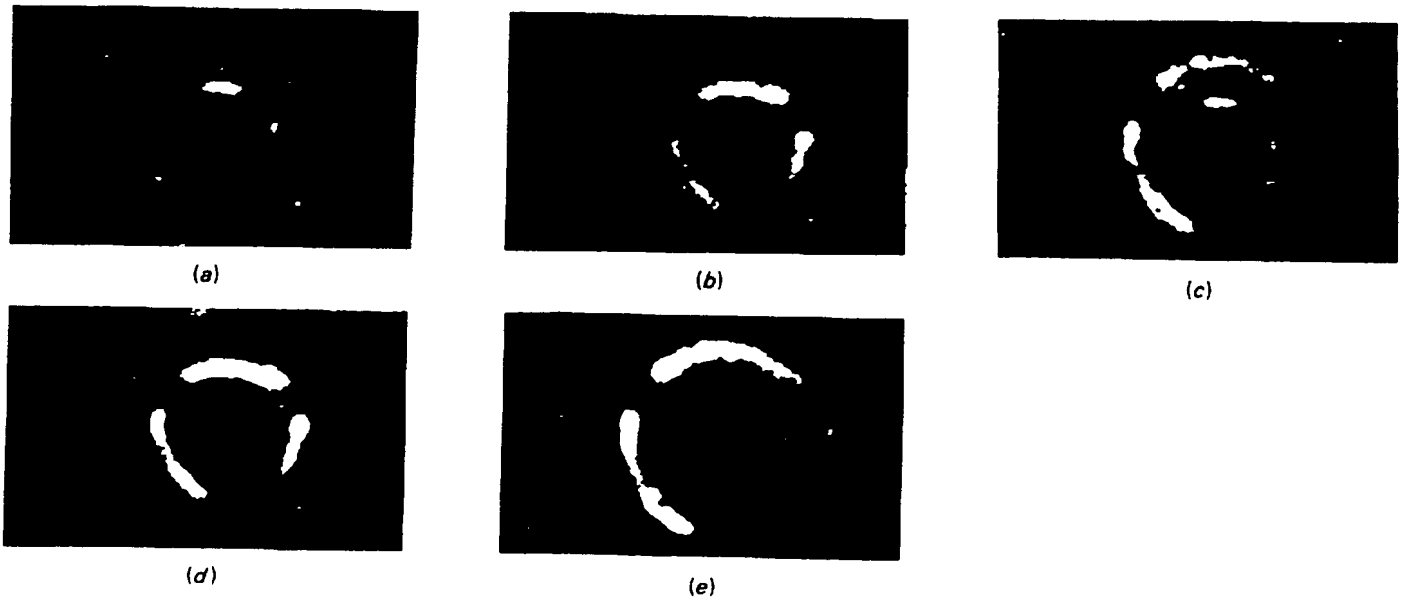

Figure 7. Pictures of the intensity distribution of the Ar3p lines at 5 eV pass-energy. The 2nd stage aperture of the CMA is removed. From (*a*) to (*e*) the kinetic energy increases.

and a temperature of 40 K is now easily reached. This limits the azimuthal range to ±90°.

Photons are produced in a home-built He resonance lamp with a 50 mm long burning tube ($\varphi_{ins} = 1$ mm) using two-stage differential pumping. The lamp assembly is fitted by means of a bellows to the vacuum chamber, so that it is easily aligned. The He gas is purified in a cooled zeolite trap. A stable discharge is maintained at 600 V and up to 50 mA without cooling. The lamp is especially suited for HeI radiation and gives 10^3 and 2×10^3 counts/s at respectively 5 and 10 eV pass-energy on the $Ar2p_{3/2}$ line (pressure 2×10^{-5} Torr (2.66 mPa)). For polycrystalline Au we obtain, in the top of the valence band, 2×10^3 and 10^4 counts/s at respectively 5 and 10 eV pass-energy. The HeII intensity is about a factor 100 lower.

The vacuum system is pumped with a four stage oil diffusion pump which is trapped with a liquid nitrogen cooled baffle. After a mild bake-out a pressure of 2×10^{-10} is easily obtained.

4. Experimental results

To study the obtainable resolution, spectra were recorded of the Ar3p lines at different pass-energies. The spectra are shown in figure 5. As is well known (Turner *et al* 1970), these lines have a very low intrinsic width of 2–3 meV. The spectra are recorded from a small segment of the circular image. The spectra of figure 5 clearly show the Ar3p spin–orbit splitting, which was unobservable before we coated the analyser with graphite and replaced the grids on the inner cylinder. The experimental resolution (full width at half maximum (FWHM)) at respectively 5, 10 and 15 eV pass-energy was 50, 90 and 140 meV, giving $\Delta E/E \simeq 0.9\%$. Theoretically the FWHM can be calculated from the full energy response function, as is done for instance by Draper and Lee (1977). This is however beyond the scope of this work. We also give the HeI spectrum of H_2 in figure 6, where it is seen that the vibrational splittings are clearly resolved.

To demonstrate the resolving power, we show in figure 7 some photographs of the intensity distributions of the Ar3p lines at different kinetic energies. The pictures are taken directly from the phosphorescent screen that was used in place of the resistive anode detector. In this experiment we decreased the energy resolution by removing the 2nd stage exit diaphragm, which results in an opening of about 15 mm diameter (standard 0.8 mm). The pass-energy is 5 eV. Between the analyser exit and the first channel plate, a constant accelerating voltage is used. The three interruptions in the image are due to the bars that hold the grids on the inner cylinder. Now both the $Ar3p_{1/2}$ and the $Ar3p_{3/2}$ electrons pass the analyser, although they still are resolved in the plane of the flat detector, and give rise to two circular images with distinct intensities. For instance in figure 7(*c*), the inner image corresponds to the $Ar3p_{3/2}$ electrons and the outer one to $Ar3p_{1/2}$ electrons. This opens the possibility to use the CMA dispersion during the accumulation of a spectrum for also simultaneous energy dependent measurement. When the analyser is operated with 50 eV pass-energy a 3 eV wide region of the spectrum can be monitored simultaneously at the detector, giving a considerable increase in sensitivity. It is noted that because of the use of an extended source, the sample should be positioned accurately. Field penetration in the large exit opening can be eliminated with a grid at this place. The images in figure 7 are seen to be slightly distorted from a circular shape, in particular at onset. We attribute this to slight misalignments and irregularities in the grids.

To demonstrate the possibility of taking angle-resolved photoelectron spectra, we show in figure 8 spectra, taken in the ΓLU plane of the Ag(111) surface. The crystal is oriented with Laue back reflection and by comparing these spectra with those reported in the literature. The surface is cleaned by Ar^+ ion

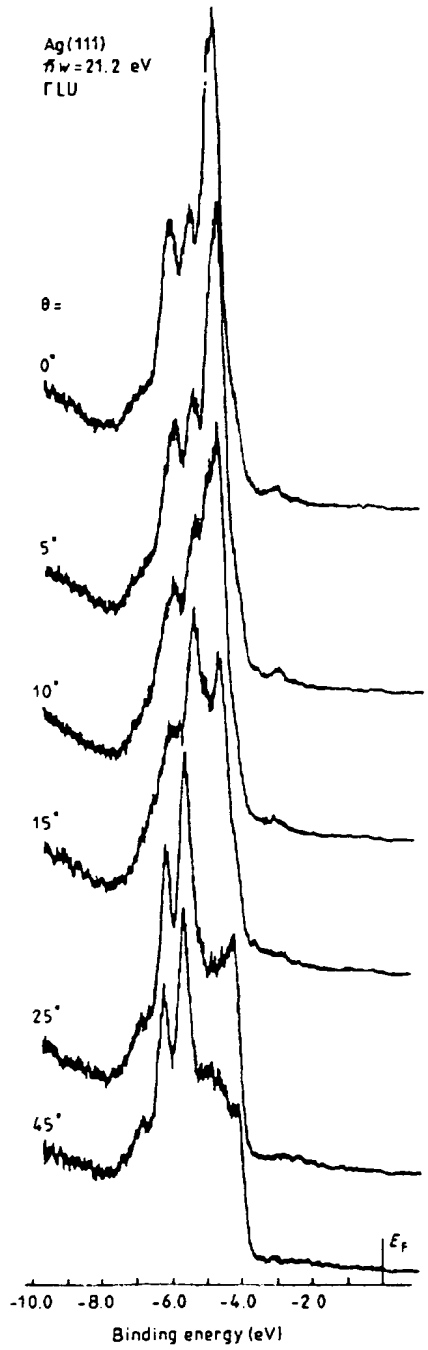

Figure 8. Angle-resolved photoelectron spectra of Ag(111) in the ΓLU plane.

etching and annealing. The pass-energy is 15 eV and the resolution 0.14 eV. In the figure, the spectra are shown as functions of the polar exit angle θ_e by rotating the sample.

With the spectra of figure 8, an estimate can be made of the angular resolution. The spectra are recorded from a small segment selected in the circular image, however without limiting the radial extend. This results in an uncertainty at the detector of $\Delta\varphi_e = \pm 3°$. The various contributions to the angular uncertainty are given in table 1.

From figure 8 we estimate $\Delta\theta_e$ to be approximately ±2.5°.

Table 1. Contributions to the angular spread in degrees.

	$\Delta\theta$	$\Delta\varphi$
Acceptance solid angle	± 6.0	
Exit aperture	± 1.0	± 1.8
Source		± 0.9
Detector		± 3.0

5. Conclusions

It is shown that the cylindrical mirror analyser, used in combination with a position sensitive detector, can be employed as a versatile angle-resolving spectrometer. This is demonstrated in the angle-resolved photoelectron spectra of Ag(111). When the full angular range, which is available in the CMA acceptance solid angle, is recorded, multiple angle-resolved spectra can be obtained simultaneously.

When the 2nd stage exit aperture is taken large a fairly wide energy region of the spectrum can be monitored at the detector. This may give a considerable increase in sensitivity of the instrument.

References

Aksela S, Karras M, Pessa M and Suoninen E 1970 Study of the electron optical properties of an electron spectrograph with coaxial cylindrical electrodes
Rev. Sci. Instrum. **41** 351

Baird R J 1981 Angle-resolved photoemission from CO chemisorbed on Rh (110)
J. Electron. Spectrosc. Rel. Phenom. **24** 55

Bosch A J 1982 Photoelectron spectroscopy. New angle-resolved spectrometer and study of dilute alloys
Thesis Groningen

Draper J E and Lee Cheng-Yi 1977 Response functions of ring-to-axis, axis-to-axis and $n = 1.5$ cylindrical mirror analysers with finite source and slit and central angle 30°–65°
Rev. Sci. Instrum. **48** 852

Eagen C F and Sichafus E N 1977 Transmission properties of a cylindrical mirror analyzer viewed in energy-angle space
Rev. Sci. Instrum. **48** 1269

Eastman D E, Donelon J J, Hien N C and Himpsel F J 1980 An ellipsoidal mirror display analyzer system for electron energy and angular measurements
Nucl. Instrum. Meth. **172** 327

Gremmelmaier R 1952
These Karlsruhe

Harting E 1971 A combined energy and angle analyzer for scattered electrons
Rev. Sci. Instrum. **42** 1151

van Hoof H A and van der Wiel M J 1980 Position-sensitive detector system for angle-resolved electron spectroscopy with a cylindrical mirror analyser
J. Phys. E: Sci. Instrum. **13** 409

Lampton M and Carlson C W 1979 Low distortion resistive anodes for two-dimensional position-sensitive MCP systems
Rev. Sci. Instrum. **50** 1093

Niehus N and Bauer E 1975 Low energy ion back scattering spectroscopy (ISS) with a commercial Auger cylindrical mirror analyzer
Rev. Sci. Instrum. **46** 1275

Palmberg P W 1974 Combined ESCA/Auger system based on the double-pass cylindrical mirror analyzer
J. Electron. Spectrosc. Rel. Phenom. **5** 691

Sar-El H Z 1968 Cylindrical capacitor as an analyzer: II. Relativistic part
Rev. Sci. Instrum. **39** 533

Schnell R D, Rieger P and Steinmann W 1984 A two-dimensional data acquisition system for a display type electron energy analyser
J. Phys. E: Sci. Instrum. **17** 221

Turner D W, Baker A D, Baker C and Brundle C R 1970 *Molecular Photoelectron Spectroscopy* (London: Wiley)

Zashkvara V V, Korsunskii M I and Kosmachev O S 1966 The focussing properties of an electrostatic mirror with a cylindrical field
Sov. Phys.–Tech. Phys. **11** 96